day. When the parasite density becomes about 1% (one red blood cell is infected in 100 red blood cells), the mouse is anesthetized and bitten by mosquitoes.

2.5. Life cycle of malaria parasite in mosquito

In the midgut of anophline mosquito, male gametocytes start exflagellation and 8 male-gametes leave from the cell body for female gametes. Then male and female gametes fertilize and grow to zygotes and later to ookinetes. About 24 h later, matured ookinetes pass through the midgut and settle at the outside of the midgut as oocysts. 10–14 days later, each oocyst grows in size and contains thousands of sporozoites inside. Oocysts are destroyed naturally and sporozoites are released into blood stream of the mosquito. Sporozoites can specifically attach the surface of the SG and invade the SG. Finally the mosquito with the sporozoites in the SG can infect an animal when the mosquito feeds blood from the animal, because the sporozoites in the SG are injected into the skin of the animal together with saliva when the mosquito bites the animal [10].

2.6. HPLC-ECD system

We used PU-980 HPLC system from Nippon Bunko (Tokyo) wuth a column of TSKgel ODS-100S from TOSO (Tokyo), and ECD-300 from EIKOM (Tokyo).

2.7. Chemicals

All chemicals (tryptophan, kynurenine, 3-hydroxykynurenine, quinaldei acid, kynurenic acid and xanthurenic acid) were purchased from Sigma-Aldrich Co (St Louis, USA).

2.8. HPLC-ECD wave-patterns of tryptophan and its derivatives

HPLC was performed as described elsewhere [11]. To compare the wave of XA with those of other tryptophan derivatives, XA and one of the derivatives were mixed, applied on HPLC-ECD system and the wave-patterns were recorded.

2.9. Measuring of XA content in adult and mosquito tissues

Mosquitoes were killed by freezing and crushed in a plastic tube with 0.5 ml of 0.4 M formic acid. For SG, 10 to 20 pairs were dissected and collected in a plastic tube. Each sample was sonicated on ice for 2 minutes and centrifuged for 15 minutes at 2000 g. The supernatants were ultrafiltrated through a series of molecular weight cut-off filters of 100, 30 and 5 kDa (VivaScience AG, Hannover, Germany). Filtrated samples were applied for HPLC-ECD system. For drawing standard line of XA, pure and flesh XA solutions with different concentration were prepared on each day and applied on HPLC-ECD system. We compared the standard line with the height of the XA peak obtained from the mosquito samples, and estimated XA content in each sample.

Please cite this article as: H. Matsuoka et al., The role of tryptophan and its derivatives for development of malaria parasite in vector mosquito, Int. Congr. Ser. (2007), doi:10.1016/j.ics.2007.07.033

2.10. Comparison of young mosquitoes with old mosquitoes

Pupa were collected and put in a nylon-meshed cage with 30 cm cube. They emerged 1–2 days later. Emergence day was recorded in each cage. Adult mosquitoes were collected from the cages and used in each experiment. For instance, to compare transmission efficacy between young mosquito group (2–3 days after emergence) and old mosquito group (12–14 days after emergence), mosquitoes were moved to pots with nylon mesh, from which they could feed a mouse. Two groups of mosquitoes were allowed to feed from the same mouse infected with *P. berghei*. Unfed mosquitoes were removed. Twelve days later, the mosquitoes were dissected and the number of oocysts developed on the midgut was counted.

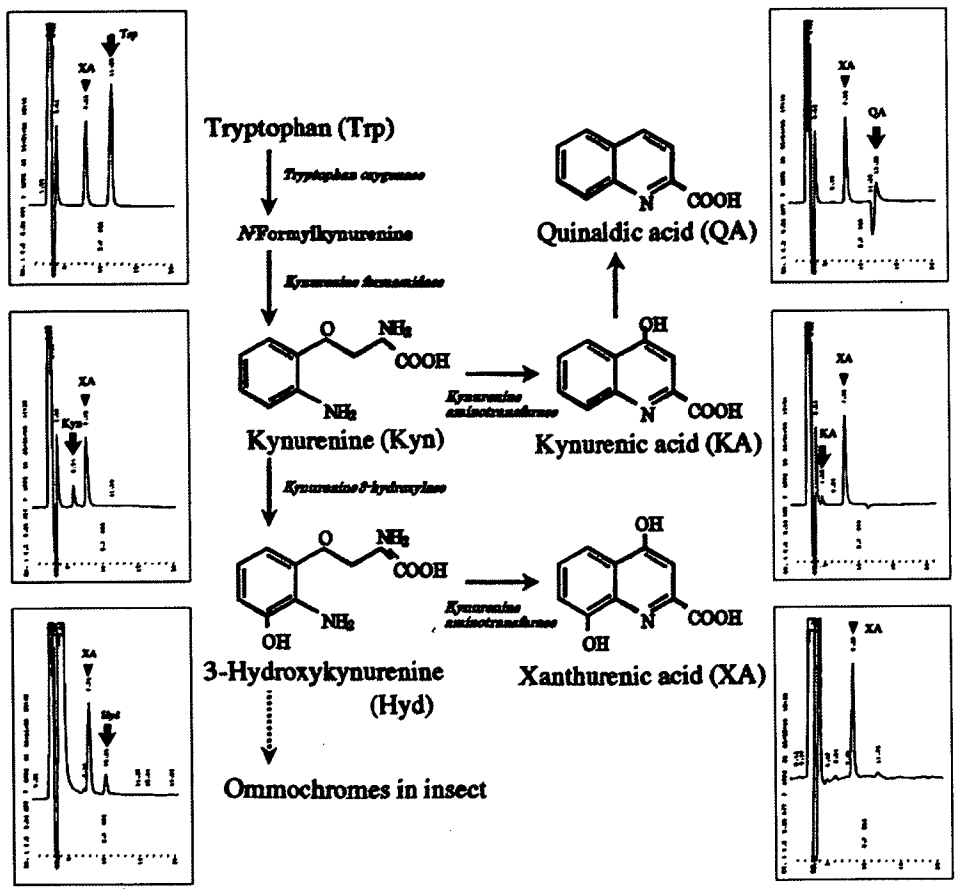

Fig. 1. The ommochrome biosynthesis pathway of tryptophan (Trp) with chemical structures of the intermediates: kynurenine (Kyn), 3-hydroxykynurenine (Hyd), quinalic acid (QA), kynurenic acid (KA) and xanthurenic acid (XA). Wave patterns of XA and each of intermediate were recorded after applying on HPLC-ECD system. Some intermediate steps from Hyd to ommochrome are omitted.

Please cite this article as: H. Matsuoka et al., The role of tryptophan and its derivatives for development of malaria parasite in vector mosquito, Int. Congr. Ser. (2007), doi:10.1016/j.ics.2007.07.033

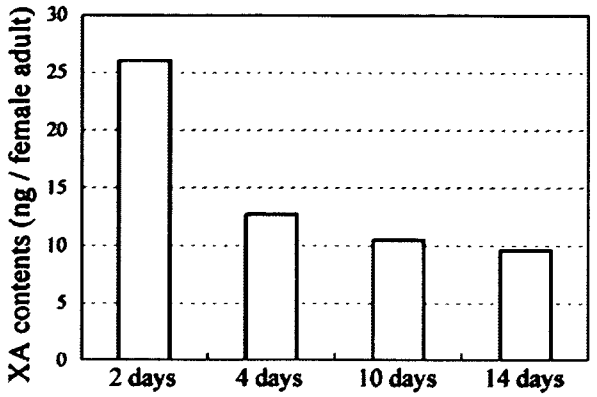

Fig. 2. XA content in whole body of adult mosquitoes. Five female adult mosquitoes with the different days after emergence were collected, homogenized, sonicated, filtrated and applied on HPLC-ECD system to estimate XA content. Column represents XA content of one female adult mosquito in each age group.

2.11. Ookinete culture

Ookinetes were cultured with the methods described by Winger et al. [12].

2.12. Membrane feeding

Cultured ookinetes were given to mosquitoes through parafilm using membrane feeding method, see Harada et al. [13]. Young and old mosquitoes were collected in each pot with nylon mesh, from which they could feed. Both groups of mosquitoes were allowed to feed the same material of cultured ookinetes. Unfed mosquitoes were removed. Twelve days

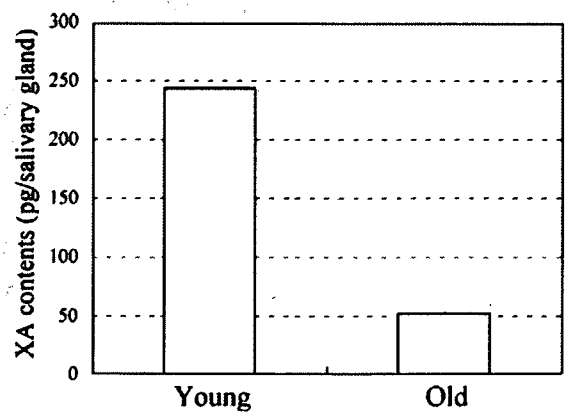

Fig. 3. XA content in the salivary gland (SG) of young and old mosquitoes. Twenty pair of SG were collected, sonicated, filtrated and applied on HPLC-ECD system to estimate XA content. Column represents XA content of one pair of SG in each mosquito group.

Please cite this article as: H. Matsuoka et al., The role of tryptophan and its derivatives for development of malaria parasite in vector mosquito, Int. Congr. Ser. (2007), doi:10.1016/j.ics.2007.07.033

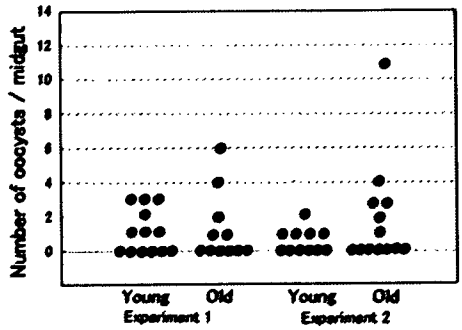

Fig. 4. Comparison of transmission efficacy between young (2–3 days after emergence) and old (12–14 days after emergence) mosquitoes. Numbers of oocyst on the midgut are plotted. In each experiment, both mosquito groups had fed on the same mouse infected with malaria.

later, the mosquitoes were dissected and the number of oocysts developed on the midgut was counted.

3. Results

The ommochrome biosynthesis pathway of tryptophan (Trp) is shown in Fig. 1. Wave patterns of xanthurenic acid (XA) and each of intermediate such as kynurenine (Kyn), 3-hydroxykynurenine (Hyd), quinalic acid (QA), kynurenic acid (KA) were recorded after applying on HPLC-ECD system. The wave of each intermediate appeared at the different place from that of XA.

As shown in Fig. 2, XA content of female adult was highest at day 2 after emergence. The content decreased gradually, and on day 14 XA level decreased by one third compared with the level on day 2. Similar tendency was observed in the SG (Fig. 3). XA content was 245 pg in the young mosquito group (2–3 days after emergence) and 53 pg in the old

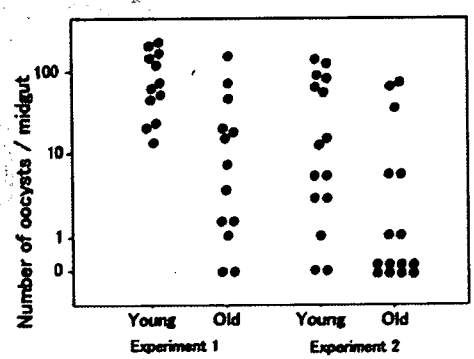

Fig. 5. Comparison of transmission efficacy between young (2–3 days after emergence) and old (12–14 days after emergence) mosquitoes. Numbers of oocyst on the midgut are plotted. In each experiment, both mosquito groups had fed cultured ookinetes by membrane feeding method.

Please cite this article as: H. Matsuoka et al., The role of tryptophan and its derivatives for development of malaria parasite in vector mosquito, Int. Congr. Ser. (2007), doi:10.1016/j.ics.2007.07.033

mosquito group (12–14 days after emergence). Thus, young adult female stores about five times more XA in the SG comparing with old female.

We compared transmission efficacy between young and old mosquito groups. Both groups of mosquitoes fed on the same mouse infected with malaria parasites. The numbers of oocyst developed on the midgut were more in the young group than those in the old group (Fig. 4). In the next experiment, we let two groups of mosquitoes feed cultured ookinetes through parafilm membrane. There was no difference in the numbers of oocyst on the midgut in both groups (Fig. 5).

4. Discussion

In the previous study [11], we added tryptophan in suger meal for adult mosquitoes as the source of XA. Accordingly the total amount of XA increased in the whole body of adult mosquitoes, however in the SG, the amount of XA did not increase but decreased by a half of the control mosquitoes. We could not explain such a biased distribution of XA. Next we allowed both mosquito groups to feed on the same mouse infected with malaria, and dissected the mosquitoes 12 days later to count the number of oocysts on the midgut. The numbers of oocyst were less in the group which had taken tryptophan meal. This indicates that transmission efficacy is controlled not by total amount of XA in the whole body but by the amount of XA in the SG.

In the present study, we compared young mosquitoes with old mosquitoes for transmission efficacy. Young mosquitoes contained larger amount of XA in the SG as well as in the whole body compared with those in old mosquitoes. Although both groups of mosquitoes fed on the same mouse infected with malaria, the numbers of oocyst in the young group were higher than that in the old group. This was an expected result. Because the young mosquitoes contained more XA in the SG, and more XA transferred from the SG to the midgut. Then XA reacted with male gametocytes in the midgut, and finally more ookinetes developed and settled outside of the midgut as oocysts. When both groups fed cultured ookinetes, the numbers of oocyst developed outside of the midgut were similar between both groups. These results suggest that conditions for development from ookinetes to oocysts are similar in both young and old mosquitoes, but the first condition, the amount of XA in the SG, affects transmission efficacy.

In field conditions, more than 90% of mosquitoes coming for blood feeding are young mosquitoes. After emergence, female mosquitoes mate with male mosquitoes and come to human or animals for blood feeding. Estimating age is 1–3 days old after emergence. This period should be shorter for mosquitoes living in the field. If it is longer, they lose their lives by heavy rain, strong wind and other insects or animals. In terms of the life cycle of malaria, mosquitoes take blood at the best timing for male gametocyte, because XA content in the SG is highest in this period.

After recognizing these results, we should be aware of the mosquito's age when we use mosquitoes in laboratory experiments. If we evaluate transmission blocking efficacy of some medicines or some vaccine candidate proteins, for instance, we should use mosquitoes of the same age; otherwise we will obtain biased results.

Please cite this article as: H. Matsuoka et al., The role of tryptophan and its derivatives for development of malaria parasite in vector mosquito, Int. Congr. Ser. (2007), doi:10.1016/j.ics.2007.07.033

Acknowledgments

We thank Mrs. Chisato Seki, Mrs. Maiko Minari, Mrs. Junko Yamamoto and Miss Maiko Nakamura for maintaining mosquitoes in our laboratory. This work was supported by a grant from Japan KEIRIN Association.

References

[1] M.M. Nijhout, *Plasmodium gallinaceum*: exflagellation stimulated by a mosquito factor, Exp. Parasitol. 48 (1979) 75–80.

[2] O. Billker, et al., The roles of temperature, pH and mosquito factors as triggers of male and female gametogenesis of *Plasmodium berghei* in vitro, Parasitol 115 (Pt 1) (1997) 1–7.

[3] E. Luo, et al., Changes in the salivary proteins during blood feeding and detection of salivary proteins in the midgut after feeding in the malaria vector *Anopheles stephensi* (Diptera: Culicidae), Med. Entomol. Zool. 51 (2000) 13–20.

[4] M. Hirai, et al., Characterization and identification of exflagellation-inducing factor in the salivary gland of *Anopheles stephensi* (Diptera: Culicidae), Biochem. Biophys. Res. Commun. 287 (2001) 859–864.

[5] J. Wang, M. Hirai, S. Yoshida, M. Arai, A. Iahii, H. Matsuoka, Comparison of malaria parasite gametocyte activating factor in the salivary glands of five species of mosquito (Diptera: Culicidae), Med. Entomol. Zool. 53(3): 177–82. Q2

[6] O. Billker, et al., Identification of xanthurenic acid as the putative inducer of malaria development in the mosquito, Nature 392 (1998) 289–292.

[7] G.E. Garcia, et al., Xanthurenic acid induces gametogenesis in *Plasmodium*, the malaria parasite, J. Biol. Chem. 273 (1998) 12003–12005.

[8] J. Li, G. Li, Identification of 3-hydroxykynurenine and xanthurenic acid and the quantification of 3-hydroxykynurenine transaminase activity using HPLC with electrochemical detection, J. Liq. Chromatogr. Relat. Technol. 21 (1998) 1511–1523.

[9] H. Matsuoka, et al., Depletion of salivary gland proteins in *Anopheles stephensi* (Diptera: Culicidae) on blood feeding, and induction of antibody to the proteins in mice being fed, Med. Entomol. Zool. 48 (3) (1997) 211–218.

[10] H. Matsuoka, et al., A rodent malaria, *Plasmodium berghei*, is experimentally transmitted to mice by merely probing of infective mosquito. *Anopheles stephensi*, Parasitol. Int. 51 (1) (2002) 17–23.

[11] B.A. Okech, M. Arai, H. Matsuoka, The effects of blood feeding and exogenous supply of tryptophan on the quantities of xanthurenic acid in the salivary glands of *Anopheles stephensi* (Diptera: Culicidae), Biochem. Biophys. Res. Commun. 341 (4) (2006) 1113–1118.

[12] L.A. Winger, et al., Ookinete antigens of Plasmodium berghei. Appearance on the zygote surface of an Mr 21 kD determinant identified by transmission-blocking monoclonal antibodies, Parasite Immunol. 10 (2) (1988) 193–207.

[13] M. Harada, H. Matsuoka, S. Suguri, A convenient mosquito membrane feeding method, Med. Entomol. Zool. 47 (1) (1996) 103–105.

Please cite this article as: H. Matsuoka et al., The role of tryptophan and its derivatives for development of malaria parasite in vector mosquito, Int. Congr. Ser. (2007), doi:10.1016/j.ics.2007.07.033

Available online at www.sciencedirect.com
ScienceDirect
Biochemical and Biophysical Research Communications 365 (2008) 758–763
BBRC
www.elsevier.com/locate/ybbrc

Antigen-specific CD8$^+$ T cells induced by the ubiquitin fusion degradation pathway

Takashi Imai, Xuefeng Duan, Hajime Hisaeda, Kunisuke Himeno *

Department of Microbiology and Immunology, Graduate School of Medical Sciences, Kyushu University, Fukuoka 812-8582, Japan

Received 6 November 2007
Available online 20 November 2007

Abstract

We have developed a DNA vaccine encoding a fusion protein of ubiquitin (Ub) and target proteins at the N-terminus for effective induction of antigen-specific CD8$^+$ T cells. A series of expression plasmids encoding a model antigen, ovalbumin (OVA), fused with mutated Ub, was constructed. Western blotting analyses using COS7 cells transfected with these plasmids revealed that there were three types of amino acid causing different binding capacities between Ub and OVA. Natural Ub with a C-terminal glycine readily dissociated from OVA; on the other hand, artificially mutated Ub, the C-terminal amino acid of which had been exchanged to valine or arginine, stably united with the polypeptide, while Ub with a C-terminal alanine partially dissociated. The ability of DNA vaccination to induce OVA-specific CD8$^+$ T cells closely correlated with the stability of Ub fusion to OVA. Our strategy could be used to optimize the effect of genetic vaccines on the induction of CD8$^+$ T cells.

Keywords: Ubiquitin; Ubiquitin fusion degradation pathway; CD8$^+$ T cells; DNA vaccine

CD8$^+$ T cells play important roles as cytotoxic T lymphocytes (CTLs) in the elimination of infectious pathogens, tumors and transplanted tissues. Antigenic peptides presented by major histocompatibility complex (MHC) class I molecules on the surface of antigen-presenting cells (APCs), and recognized by CD8$^+$ T cells, are proteolytically produced by the ubiquitin-proteasome system (UPS) [1,2].

The UPS comprises two discrete steps: the covalent attachment of multiple ubiquitin (Ub) molecules to a protein substrate, and recognition/degradation of polyubiquitinated proteins by the proteasome complexes [3]. The attachment of the first Ub to substrate occurs under stringent regulation to selectively degrade unfolded/harmful proteins, although Ub conjugation to substrates is reversible in some cases. Once the first Ub is attached, a polyUb chain is rapidly formed according to recognition signal for the proteasomes. Thus, ubiquitination of the substrate is the rate-limiting step of protein degradation by the UPS.

Ubiquitinated proteins destined for destruction are often rescued by detaching Ub with deubiquitination enzymes [4,5]. To potentiate the degradation of target protein by the proteasome, previous work has developed artificially fused proteins bearing mutated N-terminal Ub moieties. This proteolytic system is termed the Ub fusion degradation pathway (UFD). The UFD bypasses the unpredictable attachment of the first Ub to the lysine residues of substrates by fusing Ub to the N-terminus of a substrate in a non-removable fashion to provide a scaffolding for the polyUb chain. The UFD approach has as its basis the mutation of the C-terminal glycine residue of Ub to an alanine or valine to prevent cleavage by deubiquitination enzymes, such that Ub remains fused to the protein after translation [6–9]. This approach has been applied to genetic vaccines to effectively induce CTL responses by enhancing the production of antigenic peptides presented by MHC class I molecules [10–12]. However, the mutation strategy to construct non-removable Ub is based on previous

* Corresponding author. Fax: +81 (0) 92 642 6118.
E-mail address: imai@parasite.med.kyushu-u.ac.jp (K. Himeno).

0006-291X/$ - see front matter © 2007 Elsevier Inc. All rights reserved.
doi:10.1016/j.bbrc.2007.11.034

studies using yeast [6–9], and it was not clear whether this new technology would be applicable to mammals.

In this study, we constructed expression plasmids encoding ovalbumin (OVA) fused to mutated Ub with a modified C-terminal amino acid, to analyze the influence of the stability of Ub fusion to OVA on the induction of OVA-specific $CD8^+$ T cells in the UFD system. According to transfections of COS7 cells with these plasmids, the C-terminal amino acid of Ub defined the high-, intermediate- and low-sustainability of Ub fusion. Genetic immunization of mice with these plasmids revealed that OVA-specific $CD8^+$ T cells were activated more consistently with an increase in the stability of Ub fusion to OVA. These results indicate that activation of CTLs by the UFD was improved by stabilizing Ub fusion to target antigens.

Materials and methods

Plasmid constructs. The cytosolic form without signal sequence of OVA open reading frame was isolated from the pKEz–OVA plasmid [13], which was a generous gift from Dr. Y. Itoh (Shiga University), by PCR amplification. The fragment was inserted between 5′ XhoI and 3′ AflII restriction sites of the pcDNA3.1 (−) vector (Invitrogen). The gene encoding His-tag was added between 5′ AflII and 3′ PmeI restriction sites of the pcDNA3.1 vector. To generate UbX–OVA constructs, the Ub open reading frame was isolated from a pUB vector [10] that we constructed. That was introduced between 5′ NheI and 3′ XhoI restriction sites. The C-terminal glycine residue of Ub was mutated to all other amino acids using PCR-mutagenesis. Plasmid DNA was prepared using endotoxin-free plasmid mini- and maxi-prep kits (Sigma). All constructs were confirmed by DNA sequencing.

Western blotting. COS7 cells were transfected with either pOVA or UbX–OVA plasmid vector by using lipofectamine (Invitrogen) with or without the proteasome inhibitor epoxomicin (Sigma). Twenty-four hours after transfection, Western blotting was performed as described before [10]. Anti-His (Sigma, USA) was used as the first antibody, and peroxidase-conjugated anti-mouse IgG (H + L) (Zymed Laboratories) was used as the second antibody.

Mice and DNA vaccination. C57BL/6 mice purchased from Kyudo, OVA-TCR transgenic mice (OT-I) were provided by Dr. K. Yui (Nagasaki University); Ly5.1C57BL/6 mice were from Sankyo Lab Service under permission of Dr. H. Nakauchi (Tokyo University). All experiments using mice were reviewed by the Committee for the Ethics on Animal Experiment in the Faculty of Medicine, and carried out under the control of the Guidelines for Animal Experiment in the Faculty of Medicine, Kyushu University and the Law (No. 105) and Notification (No. 6) of the Government. We used a Helios gene gun system (Bio-Rad Laboratories, USA) as described previously [10]. Mice were immunized two times with 6 μg of plasmid, at 7-day intervals.

In vivo T cell division assay. $CD8^+$ T cells from OT-I mice recognize H-$2K^b$ restricted peptide ($OVA_{257-264}$: SIINFEKL). $CD8^+$ T cells from OT-I (10^7 cells/ml) were incubated with 10 μM CFSE (carboxyfluorescein succinimidyl ester, Molecular Probes, Eugene, OR) in PBS for 15 min at 37 °C. CFSE staining was stopped by adding excess RPMI 1640 media supplemented with 10% fetal bovine serum and washing cells three times with medium. Eight million CFSE-labeled cells were adoptively transferred via an intravenous route into Ly5.1 mice. The recipient mice were subsequently immunized with pcDNA, OVA and Ub–OVA vectors. After an additional 84 h, the mice were killed and draining lymph nodes were harvested for flowcytometric analysis. Cells were stained with anti-Ly5.2 to discriminate OT-I (Ly5.2) cells from Ly5.1 cells. Stained cells were analyzed by FACS Caliber (Becton–Dickinson) and the list data were analyzed using CellQuest pro software (Becton–Dickinson). Ly5.2 cells were gated and CFSE labeling was assessed for OVA-specific T cell division.

In vivo cytotoxicity assay. Spleen cells from C57BL/6 mice were separated into two groups. One group was pulsed with an OVA-epitope peptide, SIINFEKL, and stained with 10 μM CFSE; the other group, as a reference, was stained with 1 μM CFSE using above-mentioned method. Equal numbers (8×10^6) of the two target populations were mixed and injected i.v. into the recipient Ly5.1 mice. Eighteen hours after immunization with Ub–OVA plasmid vector, single-cell suspensions from spleen were prepared and the proportions of differentially CFSE-labeled target cells were assessed by flow cytometry. The percent-specific lysis was calculated using the equation: percent-specific lysis = 100 − (% survival in peptide-pulsed cells/% survival in unpulsed cells) × 100.

Tumor challenge. Mice were challenged with 2×10^5 OVA transfected thymoma cells (EG7) injected s.c. into the back, 1 week after the last immunization. Tumor size was measured twice a week using calipers.

In vivo depletion of T cell subsets. Anti-CD4 mAb (clone GK1.5) or anti-CD8 mAb (clone 2.43) was injected intra-peritoneally, at 0.5 mg per mouse, on days −1, +14 and +28 of the tumor challenge. Tumor cells were inoculated on day 0. Depletion of each T cell subset was confirmed by flow cytometry; >95% of the appropriate cell subset was depleted.

Determination of antibodies specific for OVA. Serum antibodies specific for OVA were measured by ELISA using 96-well micro titer plates coated with 50 μl of OVA (Sigma) antigen solution (5 μg/ml). Serially diluted serum samples were added to the wells and incubated at room temperature for 2 h, and then washed with PBS containing 0.05% Tween 20. Horseradish peroxidase-conjugated anti-mouse IgG (Zymed) was diluted 1:1000 and added to the well, and then incubated at room temperature for 2 h. After extensive washing, enzymatic activity was visualized using a substrate. Optical density at 415 nm was measured using a spectrophotometer.

Statistics. Statistical evaluation of the differences between experimental groups was performed using two-tailed unpaired Student's *t*-tests for all experiments except the tumor challenge, the results of which were analyzed using the Breslow–Gehan–Wilcoxon test of the Kaplan–Meier method. Probability below 0.05 was considered statistically significant.

Results and discussion

Stability of fusion between modified ubiquitin and target protein

In the studies of the UFD in yeast, the C-terminal glycine residue of Ub was originally mutated to alanine or valine to create non-removable constructs [6–9]. To optimize the fusion stability between Ub and target protein in mammalian cells, we constructed expression vectors encoding model antigen OVA fused with Ub, in which the C-terminal glycine had been replaced with various amino acids (Fig. 1A). These vectors are designated as pUbX–OVA, where X stands for the introduced amino acid.

After transient transfection of COS7 cells with these vectors in the absence or presence of a proteasome inhibitor, epoxomicin, the cells were lysed and used for Western blotting analysis. Representative results are displayed in Fig. 1B. Three types of amino acid caused different binding stabilities between Ub and OVA. First, amino acids like the original glycine resulted in full dissociation. COS7 cells transfected with pUbG–OVA express only OVA without Ub, similarly to those transfected with a vector encoding OVA alone (pOVA), indicating that Ub was removed

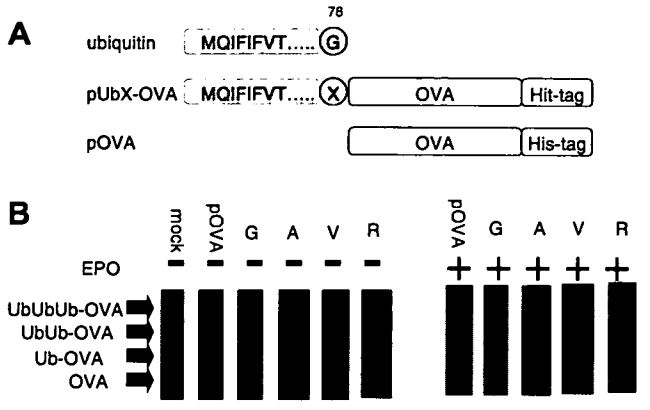

Fig. 1. Construction of plasmids encoding Ub-fused OVA. (A) Schematic presentation of the amino acid sequence of original Ub and the Ub–OVA fusion products used in this study. Note that these representations are not to scale. (B) COS7 cells transfected with the indicated plasmids were used for Western blotting using an anti-His monoclonal antibody. The amino acids indicated with a single letter code substitute the X in pUbX–OVA plasmids. The absence or presence of epoxomicin, a proteasome inhibitor, is indicated. EPO stands for epoxomicin. A result representative of 2 experiments is shown.

immediately after the UbG–OVA protein was synthesized. Second, amino acids like valine allowed no dissociation; these included arginine, aspartate, glutamate, histidine, isoleucine, proline and threonine. COS7 transfected with pUbV or pUbR–OVA contained no free OVA, but expressed a small amount of Ub–OVA, the products from the plasmids. Third, amino acids like alanine partially retained the fusion between Ub and OVA. Serine, cysteine, asparagine and glutamine are included in this group. COS7 cells transfected with pUbA–OVA showed multiple bands consisting of unconjugated OVA, UbA–OVA and oligoUb–OVA. Polyubiquitination occurred rapidly in cells transfected with pUbA–OVA.

The mutation of C-terminal glycine to alanine caused a different result between yeast and mammalian. In yeast, mutation to alanine produces ubiquitin–target fusion protein, while it produces both non-removable protein and deubiquitnated target protein in mammalian. Differences between yeast and mammalian cells might arise from differences in the quality and quantity of deubiquitination enzymes. For instance, there are at least 16 Ub-specific proteases and hydrolases in the yeast genome that catalyze the hydrolysis of peptide the bond at the C-terminal glycine of Ub [3,4], but many more such enzymes in mammalian cells [4,5].

Induction of OVA-specific CD8$^+$ T cells by DNA vaccination with pUb–OVA

Induction of antigen-specific CD8$^+$ T cells is one of the final goals in the development of effective vaccines and immunity-based therapeutic interventions against some infectious diseases, as well as against tumors. To this end, genetic vaccines utilizing the UFD have been developed to enhance the generation of antigenic peptides presented by MHC class I molecules. Some studies have succeeded in a robust amplification of CD8$^+$ T cells [10–12]. However, this type of DNA vaccine is not usually successful at effectively activating CD8$^+$ T cell responses [14,15].

We found that the C-terminal residue of Ub determines the stability of the fusion between Ub and OVA, and the feasibility of degrading OVA via the proteasome. Thus, we hypothesized that the stability of the fusion between Ub and OVA influences the ability to induce/activate OVA-specific CD8$^+$ T cells when these plasmids are used as DNA vaccines. To directly confirm this possibility, Ly5.1 congenic mice that received transfers of CFSE-labeled CD8$^+$ T cells obtained from OVA-specific T-cell receptor transgenic OT-I mice were immunized with pUb–OVA vectors. The draining axillary and inguinal lymph nodes were removed 84 h after immunization, and proliferation of transferred cells was evaluated by dilution degree of CFSE (Fig. 2A). Mice immunized with either pOVA or pUbG–OVA that expressed free OVA alone when transfected in COS7 cells (Fig. 1B), and only low grades of OVA-specific proliferation of CD8$^+$ T cells were induced in these mice. On the other hand, accelerated proliferation was observed in mice immunized with pUbA–OVA, pUbV–OVA or pUbR–OVA, all of which express a high degree of Ub–OVA compared with mice immunized with pUbG–OVA when transfected in cultured cells (Fig. 1B), indicating that polyubiquitinated OVA has the potential to highly activate OT-I CD8$^+$ T cells. Next, we evaluated the induction of OVA-specific CD8$^+$ T cells from a naïve CD8$^+$ T cell-pool after DNA immunization. C57BL/6 mice were immunized twice with Ub–OVA vectors, and spleen cells were separated in order to detect OVA-specific CD8$^+$ T cells, using a tetramer of H-2K^b–OVA epitope (Fig. 2B). Tetramer$^+$ OVA-specific CD8$^+$ T cells were significantly increased in all groups of mice immunized with OVA-expressing vectors, and the amount of increase correlated with the stability of the fusion between Ub and OVA. Immunization with pUbV or pUbR–OVA was effective in all aspects of CD8$^+$ T cell responses tested, while immunization with pOVA or pUbG–OVA was only slightly effective.

Enhanced OVA-specific cytotoxicity following immunization with pUbV or pUbR–OVA

One of the biological functions of antigen-specific CD8$^+$ T cells is the cytolytic activity targeting cells that present antigenic peptides in combination with MHC class I molecules. We examined the OVA-specific cytolytic activities of CD8$^+$ T cells using in vivo cytotoxicity assays. C57BL/6 mice were immunized with pUbX–OVA, twice, and CFSE-labeled syngeneic target cells pulsed with OVA epitope were transferred one week after immunization. Eighteen hours later, spleens were isolated and assessed by flow cytometry (Fig. 2C). As shown in Fig. 3B, induction of the cytotoxic activity of OVA-specific CD8$^+$ T cells

was closely correlated with the stable fusion of Ub to OVA. That is, mice immunized with pOVA or pUbG–OVA showed substantial cytotoxic activity against epitope-pulsed target cells, while those immunized with pUbV or pUbR–OVA showed remarkably enhanced cytotoxicity, and most target cells were killed in these mice as evaluated by in vivo cytotoxicity assay. Mice immunized with pUbA–OVA showed a significant, but low degree of cytotoxicity. Thus, vaccination with UbV fused with target protein effectively activates antigen-specific $CD8^+$ T cells.

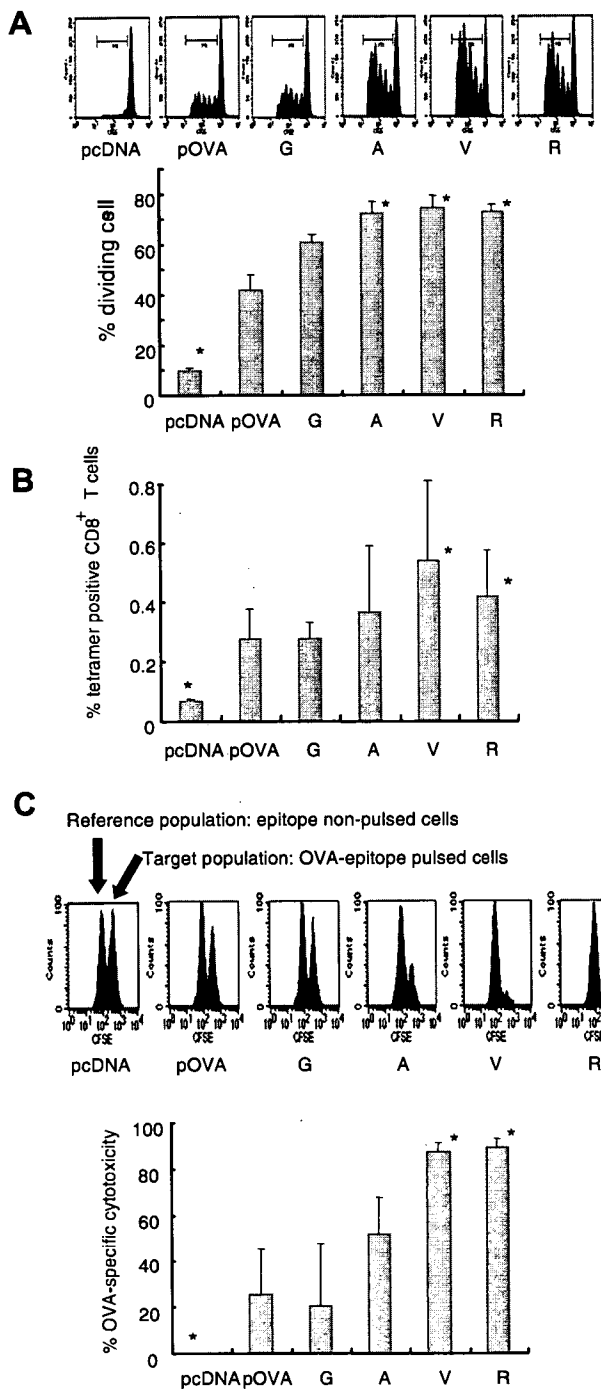

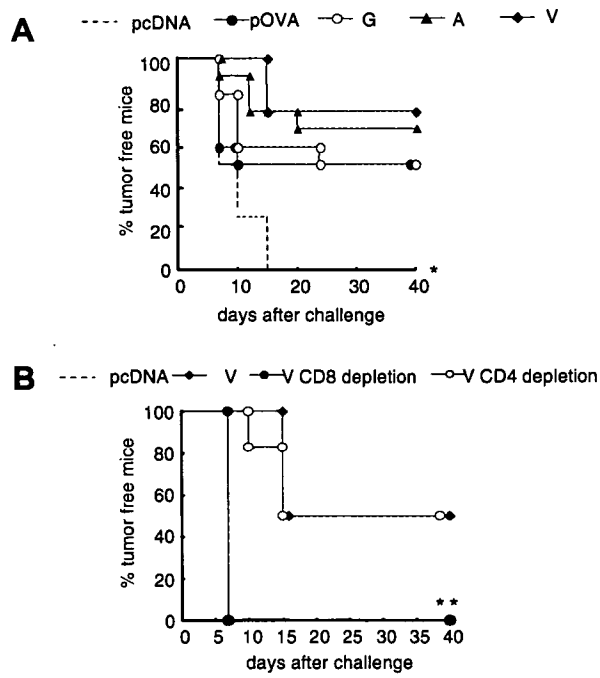

Fig. 3. Induction of protective immunity against OVA-expressing tumor in mice immunized with pUb–OVA. (A) C57BL/6 mice were vaccinated with the indicated plasmid and then challenged with EG7 cells. Tumor growth was observed twice a week. The percentage of mice that did not develop tumor is shown. Asterisks indicate statistic significance $P < 0.05$ with the Breslow–Gehan–Wilcoxon test of the Kaplan–Meier method, compared with pOVA or pUbG–OVA. (B) Critical role of $CD8^+$ T cells in the anti-tumor immunity induced in mice immunized with pUbV–OVA. $CD4^+$ or $CD8^+$ T cells were depleted from mice immunized with pUbV–OVA before the challenge with EG7. Asterisks indicate statistical significance; $P < 0.05$ with the Breslow–Gehan–Wilcoxon test of the Kaplan–Meier method compared with pUbV–OVA.

Fig. 2. Induction of OVA-specific $CD8^+$ T cells in mice immunized with pUbX–OVA. (A) Proliferation of OT-I $CD8^+$ T cells in mice after immunization. CFSE-labeled $CD8^+$ T cells from OT-I mice were transferred to Ly5.1 C57BL/6 mice. $Ly5.2^+$ cells in the draining lymph nodes were analyzed 84 hours after immunization of Ly5.1 recipients with the indicated pUbX–OVA. One representative profile of flow cytometric analyses is shown; the horizontal axis represents CFSE and the vertical axis indicates the cell number (upper panels). The percentage of dividing cells is shown (lower panel). Data are the means ± SD of three mice. (B) Induction of OVA-specific $CD8^+$ T cells in immunized mice. One week after the second immunization with the indicated plasmids, OVA-specific $CD8^+$ T cells were quantified using a tetramer of H-$2K^b$–OVA epitope complex. Data are the means ± SD of percent $tetramer^+$ cells in $CD8^+$ T cells from three mice. (C) Induction of OVA-specific cytotoxicity in mice immunized with pUb–OVA. One week after the second immunization with the indicated plasmids, OVA epitope-pulsed target spleen cells labeled with lower concentrations of CFSE and non-target spleen cells labeled with higher concentrations of CFSE were transferred. Eighteen hours later, CFSE-labeled transferred cells in spleen were analyzed by flow cytometry (upper panels). Percentages of specific cytotoxicity calculated as described in Materials and methods are shown. Data are the means ± SD from three to five mice in each group. Asterisks indicate statistical significance ($P < 0.05$ with the Student's unpaired t-test) compared with mice immunized with pOVA or pUbG–OVA. A result representative of two experiments is shown.

Mice vaccinated with pUb–OVA rejected an OVA-expressing tumor

The stability of the fusion between Ub and OVA influenced the ability to induce $CD8^+$ T cells. We evaluated the efficacy of vaccines to induce anti-tumor immunity. C57BL/6 mice were immunized twice with pUb–OVA plasmids, and one week later, those mice were inoculated with OVA-expressing syngeneic EL4 thymoma cells, EG7. Tumor growth was monitored by measuring tumor size (Fig. 3A). EG7 tumor cells gradually grew and formed a tumor mass within 2 weeks in all mock-immunized control mice. All immunized groups significantly suppressed tumor growth. Strikingly, most of the mice immunized with pUbV–OVA rejected the EG7 tumor. Mice immunized with pUbA–OVA showed intermediate protection. These immunizations did not protect mice from the tumor growth of parental EL4 cells, indicating the induction of OVA-specific anti-tumor immunity (data not shown).

To further confirm that OVA-specific anti-tumor immunity induced by immunization with pUb–OVA was mediated by activation of $CD8^+$ T cells, mice immunized with pUbV–OVA were treated with an anti-CD4 or anti-CD8 antibody to deplete the corresponding T cell subset prior to implantation of EG7 tumor cells. Complete depletion was confirmed by flow cytometry just before the tumor challenge (data not shown). As shown in Fig. 3B, depletion of $CD8^+$ T cells completely abolished the anti-tumor immunity induced by immunization with pUbV–OVA. By contrast, treatment with anti-CD4 antibody did not alter the suppression of tumor growth, indicating that the anti-tumor immunity induced by immunization with pUbV–OVA is dependent on OVA-specific $CD8^+$ T cells.

We found that the level of induction of OVA-specific $CD8^+$ T cells was proportional to the stability of the fusion between Ub and OVA produced from the expression plasmid used as a DNA vaccine. Non-removable Ub itself could serve as a target for polyubiquitination, enhancing recognition and degradation by the proteasome and resulting in effective presentation of CD8+ T cell-epitopes in OVA to MHC-class I molecules.

Production of OVA-specific antibody by DNA vaccination with pUb–OVA

The effect of vaccination was evaluated generally, by either antigen-specific cellular or humoral immunity. We estimated the production of OVA-specific antibody in response to vaccination with pUb–OVA. C57BL/6 mice were immunized twice with pUb–OVA plasmids, and one week later, sera from immunized animals were collected, and the level of OVA-specific IgG was measured (Fig. 4). There was no difference in the level of OVA-specific IgG production, which is dependent on OVA-specific $CD4^+$ T cells, among immunization groups. Therefore, it is noteworthy that ubiquitination of OVA does not influence the induction of OVA-specific $CD4^+$ T cells.

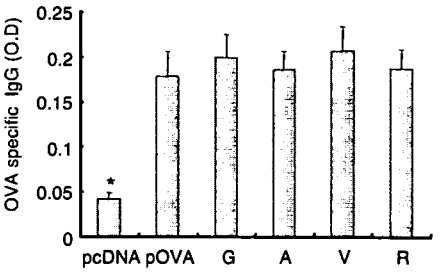

Fig. 4. Antibody responses induced in immunized mice. One week after the second immunization, serum samples collected from mice were analyzed for antibody responses specific for OVA, using ELISA. Data are the means ± SD of OD at 415 nm, of 1:400 diluted sera from six mice in each group. A result representative of two experiments is shown. Asterisks indicate statistical significance ($P < 0.05$ with the Student's unpaired t-test) compared with immunization with pOVA or pUbG–OVA.

In the present study, we showed that mutation of the C-terminal glycine residue of Ub to an amino acid such as valine or arginine is useful and essential for the development of a DNA vaccine to induce antigen-specific $CD8^+$ T cells based on the UFD. In addition to susceptibility to proteasomal degradation, the structures of target antigens may also influence the stability of Ub fusion, since mutation of the same C-terminal glycine to alanine resulted in a different outcome. That is, some antigen (lewis lung carcinoma antigen MUT1 or toxoplasma antigen SAG1) fused to UbA could induce effective $CD8^+$ T cell responses [10,11] while others such as p53 or hepatitis C virus core protein could not [14,15]; this discrepancy might be explained by differences in the stability of the fusion between Ub and the target antigenic peptides. Therefore, to further improve this type of DNA vaccine, the type of target antigen, as well as the strategy for fusion to Ub, should be considered.

Acknowledgments

This work was supported by grants from the Ministry of Education, Science Sport and Culture of Japan to K.H. (18015040, 19590429), to H.H. (18590400, 19041056), and from The Uehara Memorial Foundation to H.H.

References

[1] P.M. Kloetzel, The proteasome and MHC class I antigen processing, Biochim. Biophys. Acta 169 (2004) 5225–5233.
[2] B. Strehl, U. Seifert, E. Krüger, S. Heink, U. Kuckelkorn, P.M. Kloetzel, Interferon-gamma, the functional plasticity of the ubiquitin-proteasome system, and MHC class I antigen processing, Immunol. Rev. 207 (2005) 19–30.
[3] A.L. Schwartz, A. Ciechanover, The ubiquitin-proteasome pathway and pathogenesis of human diseases, Annu. Rev. Med. 50 (1999) 57–74.
[4] K.D. Wilkinson, Ubiquitination and deubiquitination: targeting of proteins for degradation by the proteasome, Semin. Cell Dev. Biol. 11 (2000) 141–148.
[5] C.H. Chung, S.H. Baek, Deubiquitinating enzymes: their diversity and emerging roles, Biochem. Biophys. Res. Commun. 266 (1999) 633–640.

[6] E.S. Johnson, B. Bartel, W. Seufert, A. Varshavsky, Ubiquitin as a degradation signal, EMBO J. 11 (1992) 497–505.
[7] E.S. Johnson, P.C. Ma, I.M. Ota, A. Varshavsky, A proteolytic pathway that recognizes ubiquitin as a degradation signal, J. Biol. Chem. 270 (1995) 17442–17456.
[8] T.R. Butt, M.I. Khan, J. Marsh, D.J. Ecker, S.T. Crooke, Ubiquitin metallothionein fusion protein expression in yeast, A genetic approach for analysis of ubiquitin functions, J. Biol. Chem. 263 (1998) 16364–16371.
[9] D.J. Ecker, J.M. Stadel, T.R. Butt, J.A. Marsh, B.P. Monia, D.A. Powers, J.A. Gorman, P.E. Clark, F. Warren, A. Shatzman, S.T. Crooke, Increasing gene expression in yeast by fusion to ubiquitin, J. Biol. Chem. 264 (1989) 7715–7719.
[10] X. Duan, H. Hisaeda, J. Shen, L. Tu, T. Imai, B. Chou, S. Murata, T. Chiba, K. Tanaka, H.J. Fehling, T. Koga, K. Sueishi, K. Himeno, The ubiquitin-proteasome system plays essential roles in presenting an 8-mer CTL epitope expressed in APC to corresponding CD8+ T cells, Int. Immunol. 18 (2006) 679–687.
[11] K. Ishii, H. Hisaeda, X. Duan, T. Imai, T. Sakai, H.J. Fehling, S. Murata, T. Chiba, K. Tanaka, S. Hamano, M. Sano, A. Yano, K. Himeno, The involvement of immunoproteasomes in induction of MHC class I-restricted immunity targeting Toxoplasma SAG1, Microbes Infect. 8 (2006) 1045–1053.
[12] M.A. Barry, W.C. Lai, S.A. Johnston, Protection against mycoplasma infection using expression-library immunization, Nature 377 (1995) 632–635.
[13] K. Teramoto, K. Kontani, Y. Ozaki, S. Sawai, N. Tezuka, T. Nagata, S. Fujino, Y. Itoh, O. Taguchi, Y. Koide, T. Asai, I. Ohkubo, K. Ogasawara, Deoxyribonucleic acid (DNA) encoding a pan-major histocompatibility complex class II peptide analogue augmented antigen-specific cellular immunity and suppressive effects on tumor growth elicited by DNA vaccine immunotherapy, Cancer Res. 15 (2003) 7920–7925.
[14] H. Deng, D. Kowalczyk, I. O, M. Blaszczyk-Thurin, Z. Quan Xiang, W. Giles-Davis, H.C. Ertl, A modified DNA vaccine to p53 induces protective immunity to challenge with a chemically induced sarcoma cell line, Cell Immunol. 215 (2002) 20–31.
[15] O. Vidalin, E. Tanaka, U. Spengler, C. Trepo, G. Inchauspe, Targeting of hepatitis C virus core protein for MHC I or MHC II presentation does not enhance induction of immune responses to DNA vaccination, DNA Cell Biol. 8 (1999) 611–621.

Available online at www.sciencedirect.com
ScienceDirect
Biochemical and Biophysical Research Communications 365 (2008) 621–627
BBRC
www.elsevier.com/locate/ybbrc

Ubiquitin-fusion degradation pathway: A new strategy for inducing CD8 cells specific for mycobacterial HSP65

Jianying Shen [a], Hajime Hisaeda [a], Bin Chou [a], Qingsheng Yu [b], Liping Tu [a], Kunisuke Himeno [a,*]

[a] *Department of Parasitology, Graduate School of Medical Sciences, Kyushu University, 3-1-1, Maidashi, Higashi-ku, Fukuoka 812-8582, Japan*
[b] *Division of Molecular and Cellular Immunology, Medical Institute of Bioregulation, Kyushu University, 3-1-1, Maidashi, Higashi-ku, Fukuoka 812-8582, Japan*

Received 1 November 2007
Available online 20 November 2007

Abstract

The ubiquitin-proteasome system (UPS) plays an indispensable role in inducing MHC class I-restricted $CD8^+$ T cells. In this study, we exploited UPS to induce $CD8^+$ T cells specific for mycobacterial HSP65 (mHSP65), one of the leading vaccine candidates against infection with *Mycobacterium tuberculosis*. A chimeric DNA termed pU-HSP65 encoding a fusion protein between murine ubiquitin and mHSP65 was constructed, and C57BL/6 (B6) mice were immunized with the DNA using gene gun bombardment. Mice immunized with the chimeric DNA acquired potent resistance against challenge with the syngeneic B16F1 melanoma cells transfected with the mHSP65 gene (HSP65/B16F1), compared with those immunized with DNA encoding only mHSP65. Splenocytes from the former group of mice showed a higher grade of cytotoxic activity against HSP65/B16F1 cells and contained a larger number of granzyme B- or IFN-γ-producing $CD8^+$ T cells compared with those from the latter group of mice.

Keywords: DNA vaccine; Ubiquitin-proteasome pathway; Mycobacterial HSP65

The essential role of $CD8^+$ T cells in protective immunity against *Mycobacterium tuberculosis* (MT) is being increasingly recognized [1–4]. However, vaccine trials using antigenic peptides derived from MT have met a number of questions, since those peptide vaccines rarely induce $CD8^+$ T cells.

Classical $CD8^+$ T cells recognize antigens presented to MHC class I molecules on APCs. Endogenous antigens such as oncogene products and viral products synthesized within the APC are first polyubiquitinated and then degraded into their peptide components by the proteasome. This type of antigen processing system has been generally accepted as the ubiquitin-proteasome system (UPS) [5–7]. These peptides are subsequently transported into the endoplasmic reticulum through the transporter associated with antigen processing (TAP) and then located onto MHC class I molecules. Once the antigen peptides have bound to MHC class I molecules, the peptide/MHC class I complexes are transported to the surface of the APC via the Golgi system and then the peptides are presented to the T cell receptors of $CD8^+$ T cells.

UPS is responsible for the turnover of most cellular proteins and also for the generation of the bulk of antigenic peptides presented by MHC class I molecules. In the present study, we developed a new strategy for genetic vaccination against MT by gene gun bombardment employing chimeric DNA encoding mHSP65 fused with ubiquitin at its N-terminus. The gene product is expected to be processed by the ubiquitin-fusion degradation pathway (UFD), a virtual route of the UPS [8] and then routed to

Abbreviations: APC, antigen-presenting cells; HSP65, heat shock protein 65; UPS, ubiquitin-proteaosome system; UFD, ubiquitin-fusion degradation pathway.

* Corresponding author. Fax: +81 92 642 6115.
E-mail address: himeno@parasite.med.kyushu-u.ac.jp (K. Himeno).

0006-291X/$ - see front matter © 2007 Elsevier Inc. All rights reserved.
doi:10.1016/j.bbrc.2007.11.009

MHC class I molecules, resulting in the activation of mHSP65-specific $CD8^+$ T cells. Using pHSP65 transfected B16F1 tumor cells as a challenge model, we found that a DNA vaccine encoding a ubiquitin-mycobacterial HSP65 fusion protein can induce an MHC class I-restricted protective immune response based on UPS, which provides a new strategy for designing DNA vaccines against *M. tuberculosis*.

Materials and methods

Animals and tumor cell lines. All experiments using mice were performed in accordance with the Institutional Guidelines of Kyushu University. Seven-week-old female C57BL/6 (B6) mice were purchased from Kyudo. Co., Ltd. (Tosu, Japan). The murine melanoma cell line B16F1 and its stable transfectants were maintained in PRMI1640 medium supplemented with 10% fetal bovine serum, 100 IU/ml penicillin, and 100 μg/ml streptomycin (complete medium).

Plasmids. The gene encoding mHSP65 (aa 1–540) was amplified from genomic DNA of *M. tuberculosis* strain H37Rv (NCBI Accession No. AL021932) by PCR using the following primer pair: a sense primer with an EcoRI site 5′-CCGGAATTCATGGCCAAGACAATTGCGTAC-3′ and an antisense primer with a KpnI site 5′-CGGGGTACCTCAG AAATCCATGCCACCCAT-3′. The gene encoding mouse mutant ubiquitin (Ub, aa 1–76), with the C-terminal glycine residue replaced by an alanine residue, was amplified by PCR from genomic DNA obtained from livers of B6 mice and inserted into the NheI and XhoI sites of pcDNA3.1 (−) (Invitrogen, Carlsbad, CA), and designated pU-DNA3.1. The amplified gene encoding mHSP65 was cloned into the EcoRI and KpnI sites of pcDNA3.1 or pU-DNA3.1 vector, and designated pHSP65 and pU-HSP65, respectively.

In vitro transfection and Western blotting. COS-7 cells were transfected with the mHSP65-expressing plamids by using Lipofectamine 2000 (Invitrogen) according to the product protocol and cultured for 24 h. Some of these cells were cultured with 5 μM of the proteasome inhibitor MG-132 (Calbiochem) for an additional 12 h. Cell lysates were prepared by adding lysate buffer as previously described [9]. Ten micrograms of protein was used for Western blotting. The murine monoclonal antibody IA10, specific for an epitope located between aa 172 and 224 of HSP65 from *M. bovis* (kindly provided by Dr. J. DeBruyn, Institute Pasteur de Brabant, Belgium), was used as the first antibody. Horseradish peroxidase-conjugated polyclonal antibodies to mouse IgG (Zymaed, San Francisco, CA) were used as the secondary antibody. Bound antibodies were visualized on X-ray film by enhanced chemiluminescence (Amersham Pharmacia Biotech, UK). The expression of HSP65 was quantified by densitometric analysis with LAS-1000 plus high resolution equipment (Fuji Photo Film Co., Ltd., Japan).

Establishment of stable transfectants. B16F1 cells were transfected with pHSP65 or pU-HSP65 as described above. One milligram per milliliters of G418 (Sigma, St. Louis, MO) was added 24 h after transfection. After three cycle of G418 selection, the drug-resistant cells were cloned by limiting dilution.

DNA vaccination and challenge with transfected melanoma cells. The Helios Gene Gun (BioRad, New York, NY) technique was used as described previously [9]. Briefly, plasmid DNA was precipitated onto 1.6 μm gold particles and coated onto the inner surface of the tubing by a tube loader. The final tubing segment resulted in delivery of 0.125 mg gold particles and 2 μg plasmid DNA per transfection. Each plasmid was vaccinated into three different portions of shaved abdominal skin four times at 2-week intervals. A total of 24 μg of plasmid was administered to each mouse. Two weeks after the last vaccination, 2×10^5 transfected melanoma cells in 0.1 ml PBS were implanted subcutaneously into the center of the abdomen of B6 mice. Tumor size was measured twice a week using a caliper and was calculated as $\pi/6 \times [(a \times b)^{1/2}]^3$, where a and b are two perpendicular major diameters of the tumor.

CTL assay. The cytotoxic activity was estimated by measuring the amount of fragmented DNA in target cells. The target cells, HSP65/B16F1 melanoma cells, were labeled with 2 μCi/ml of [^{3}H]thymidine overnight. These cells were collected, washed, and resuspended at a concentration of 1×10^5/ml in complete medium. Then 100 μl of this suspension was added to each well of a 96-well U-bottom plate. As effector cells, splenocytes from B6 mice two weeks after the last vaccination were stimulated with irradiated (120 Gy) melanoma cells expressing mHSP65 for 5 days, and at the second day recombinant IL-2 was added at a final concentration of 20 IU/ml. The effector cells were then collected, washed, and resuspended in the complete medium. One hundred microliters of the effector cell suspension was added to each well of the 96-well U-bottom plate at various ratios to the target cells. The plate was centrifuged for 5 min at 800*g* and then incubated for 16 h at 37 °C in 5% CO_2. After incubation the cells were frozen, thawed, and harvested onto a glass fiber filter (Packard Instrument B.V. Chemical Operations, Groningen, The Netherlands) using a 96-well harvester (Packard), and the radioactivity trapped on the filter measured with a beta counter (Packard). The percent of specific DNA fragmentation was calculated using the following formula: (spontaneous count − experimental count)/spontaneous counts × 100.

Flow cytometric analyses. One million splenocytes stimulated with 50 ng/ml PMA and 1 μg/ml ionomycin in the presence of 1 μg/ml Brefeldin A for 4 h were stained with APC-anti-CD4 (clone GK1.5, eBioscience) and PE-anti-CD8 (clone 53-6.72, eBioscience). After fixation with 4% paraformaldehyde and permeabilization with 0.1% saponin, cells were intracellularly stained with FITC-anti-IFN-γ. Similarly 1×10^6 splenocytes stimulated with 10 μg/ml of H-2^b-restricted CTL epitope derived from mHSP65 (NH2-SALQNAASIA-COOH) for 24 h were stained with FITC-anti-CD8 (eBioscience) and stained intracellularly with PE-anti-granzyme G antibody (Caltag Laboratories, Burlingame, CA). Melanoma cells expressing mHSP65 were stained with anti-mouse H-$2K^bD^b$ antibody (Cedarlane Laboratories). All stained cells were washed twice in PBS/Facs flow, and analyzed by FacsCaliber (Becton Dickinson), and the list data analyzed using Cell Quest pro software (Becton Dickinson).

Results

Construction of a chimeric DNA encoding ubiquitin-fused mHSP65

We constructed two plasmid vectors expressing mHSP65 (Fig. 1). One consisted of mHSP65 only and was termed pHSP65. The other, designated pU-HSP65, was a chimeric DNA encoding a fusion protein linking murine ubiquitin (Ub) to the N-terminus of mHSP65, thought to be processed by the UPS. Note that the C-terminal glycine of the Ub was replaced by alanine to prevent dissociation of Ub from mHSP65.

Ub-fused mHSP65 is rapidly degraded by the proteasome

To test the expression and proteasomal degradation of mHSP65 in mammalian host cells, COS-7 cells were transfected with pHSP65 or pU-HSP65 and were cultured for 12 h with a proteasome inhibitor, MG-132. Harvested cells were lysed, separated by SDS–PAGE, and subjected to immunoblotting with anti-HSP65 antibody to determine the level of protein expression (Fig. 2A). HSP90, a housekeeping protein, was also analyzed as an internal control. mHSP65 was successfully detected in COS-7 cells

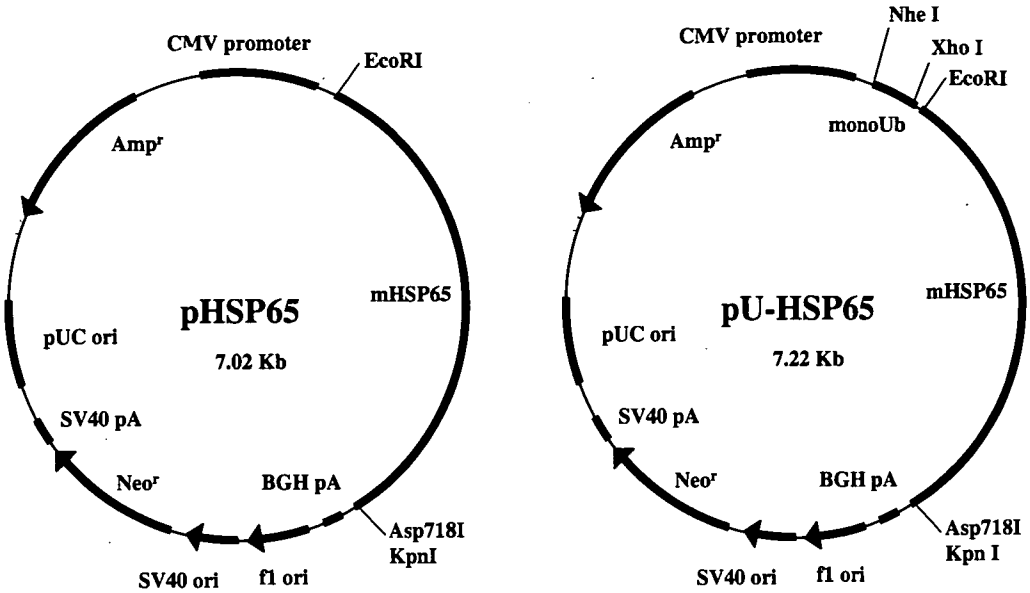

Fig. 1. Schematic representation of plasmids pHSP65 and pU-HSP65. pHSP65 or pU-HSP65-expressing mHSP65 or Ub-fused mHSP65, respectively, under the CMV promoter.

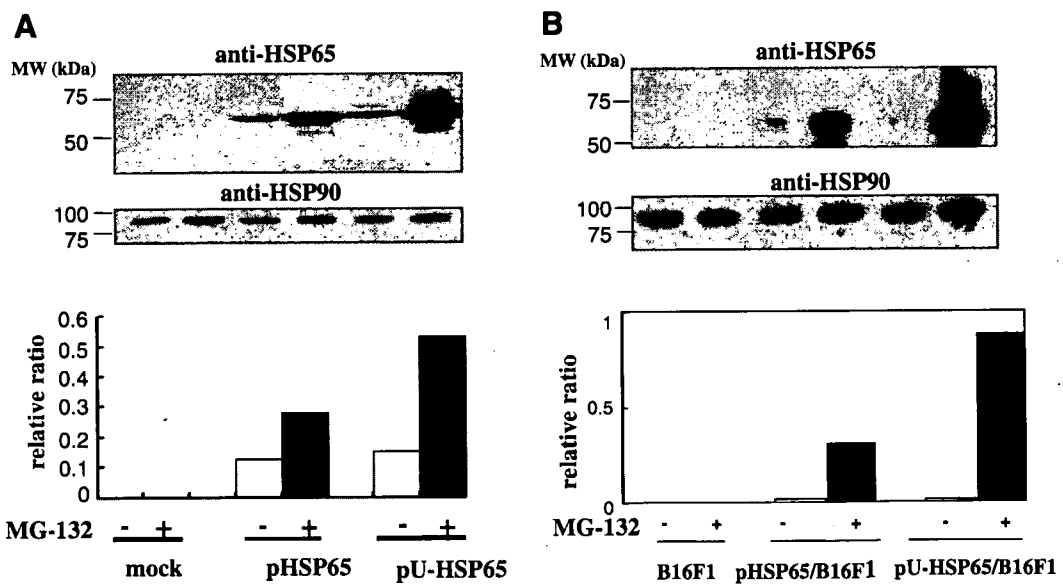

Fig. 2. Expression and proteosomal degradation of mHSP65. (A) COS-7 cells transfected with the various plasmids as illustrated were cultured in the presence or absence of MG-132. (B) Stably transfected melanoma cells cultured were cultured in the presence or absence of MG-132. Cell lysates were analyzed by immunoblotting with anti-HSP65 or anti-HSP90 monoclonal antibody. Sizes of the molecular weight markers are shown on the left in kDa. Relative expression of mHSP65 to HSP90 was calculated denstitometrically.

transfected with pHSP65, and its expression was only slightly enhanced by the inclusion of a proteasome inhibitor, MG-132. The expression level of Ub-mHSP65 in COS-7 cells transfected with pU-HSP65 was similar to that with pHSP65. However, the expression of Ub-mHSP65 was markedly enhanced in cells transfected with pU-HSP65 when MG-132 was added to the culture. Although anti-HSP65 used here recognizes mammalian HSP60, no protein was detected in mock transfected COS-7 cells, confirming that the detected protein was mHSP65.

Establishment of tumor cells stably expressing mHSP65

To evaluate induction of CTL by immunization with pU-HSP65, we tried to establish melanoma B16F1 cells expressing mHSP65. The stable transfectants were generated from B16F1 cells transfected with pHSP65 or pU-HSP65 after antibiotic-based screening and limiting dilution, and termed HSP65/B16F1 or Ub-HSP65/B16F1, respectively (Fig. 2B). As in transiently transfected COS-7 cells, expression levels of mHSP65 or Ub-mHSP65 were

comparable in the absence of MG-132, whereas Ub-mHSP65 accumulated when proteasome activity was blocked. Taken together, these results suggest that Ub-mHSP65 synthesized in the cells transfected with pU-HSP65 is promptly degraded by the proteasome.

Induction of anti-tumor immunity against melanoma expressing mHSP65 by immunization with pU-HSP65

B6 mice were immunized with pDNA, pHSP65, or pU-HSP65 and were transplanted with HSP65/B16F1 melanoma cells. Mice immunized with pHSP65 allowed rapid growth of melanoma cells in a similar manner to those with the control pDNA. In clear contrast, the enlargement of HSP65/B16F1 in mice immunized with pU-HSP65 was markedly suppressed (Fig. 3A). These immunized mice did not show suppression of the parental B16F1 melanoma cells (data not shown). Thus, immunization with pU-HSP65 induces anti-tumor immunity specific for mHSP65.

Activation of $CD8^+$ T cells in mice immunized with pU-HSP65

We examined the anti-tumor immunity mediated by $CD8^+$ T cells. $CD8^+$ T cell-dependent immunity has been shown to correlate well with cytolytic behavior and IFN-γ production. We also analyzed the induction of cytotoxic activity against mHSP65-expressing melanoma cells. Splenocytes from immunized mice were used as effector cells after stimulation with irradiated HSP65/B16F1 cells in the presence of IL-2. Cytotoxic activity against target HSP65/B16F1 cells of the effector cells from mice immunized with pU-HSP65 was prominent compared with those from the mock immunized mice, while immunization with pHSP65 did not induce any cytotoxic activity (Fig. 3B). Granzyme B is responsible for cytotoxic activity of $CD8^+$ T cells by activating apoptosis-inducing proteases in target cells. Coincident with cytotoxic activity, percentage of $CD8^+$ T cells expressing granzyme B was increased in splenocytes from mice immunized with pU-HSP65 after

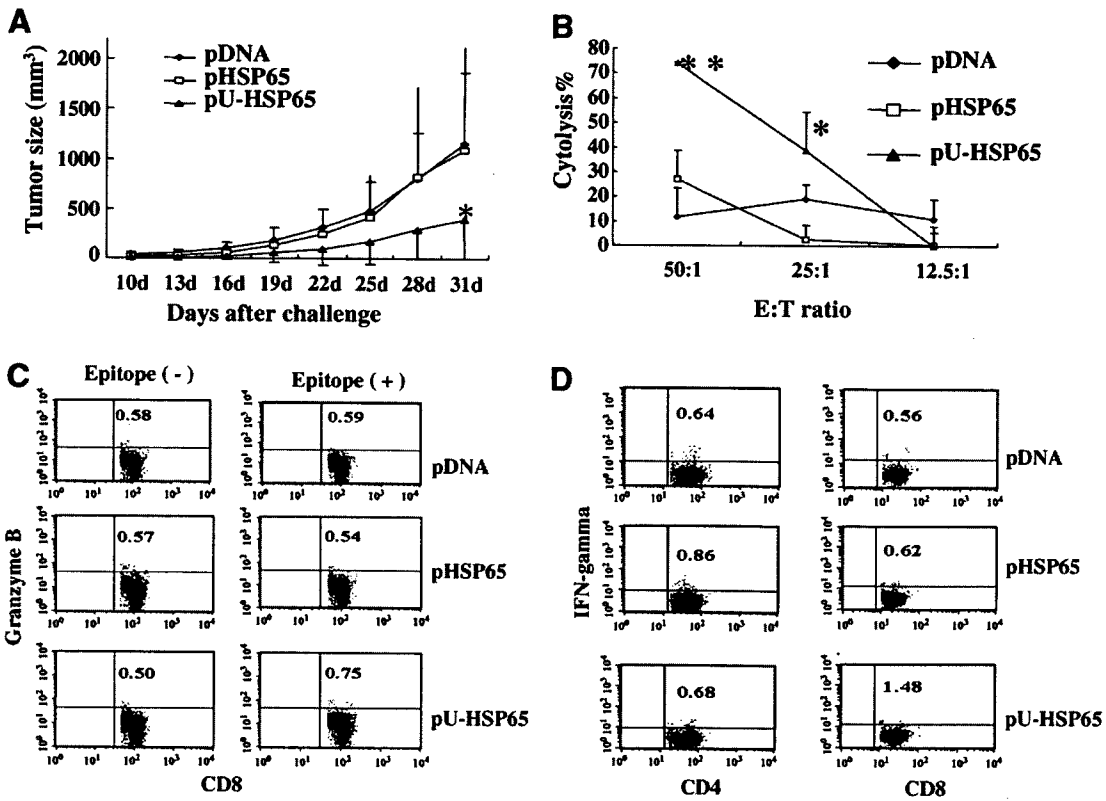

Fig. 3. Introduction of anti-tumor immunity and activation of $CD8^+$ T cells in mice immunized with pU-HSP65. (A) Induction of anti-tumor immunity against HSP65/B16 by immunization with pU-HSP65. B6 mice were immunized with the various plasmids as illustrated and challenged with HSP65/B16 cells. Tumor growth was measured every three days. Data represents mean ± one SD from five mice in each group. Asterisk indicates statistical significance at $P < 0.05$ with the Student's *t*-test compared with the other two groups. One representative result of three repeated experiments is shown. (B) CTL activity of splenocytes from mice immunized with the various plasmids as illustrated was analyzed. Effector cells were prepared from splenocytes from immunized mice after *in vitro* stimulation and were mixed with [^{3}H]thymidine-labeled HSP65/B16 target cells at the ratios shown. After a 16-h incubation, cells were harvested, radioactivity counted with a beta counter, and specific killing calculated. Double asterisks or asterisk indicate statistical significance at $P < 0.01$ or $P < 0.05$, respectively, with the Student's *t*-test compared with the other two groups. Production of granzyme B (C) and IFN-γ (D) in $CD8^+$ T cells in mice immunized with the various plasmids as illustrated were analyzed using flow cytometry. After *in vitro* stimulation of spleen cells, granzyme B or IFN-γ was stained in combination with surface staining of CD4 or CD8. The numbers represent the percentage of the corresponding quadrants.

stimulation with the H-2^b-restricted $CD8^+$ T cell epitope (Fig. 3C). This increase seems very slight, but effector $CD8^+$ T cells specific for one epitope are expected to be small. Furthermore, the percentage of IFN-γ^+ cells in $CD8^+$ T cells was markedly increased in the PMA/Ca^{2+} ionophore-stimulated splenocytes of mice immunized with pU-HSP65 compared with the other two groups (Fig. 3D). On the other hand, immunization of mice with pHSP65 did not affect the population of IFN-γ-producing $CD8^+$ T cells, although the population in $CD4^+$ T cells was slightly augmented (Fig. 3C). These results indicate that the functions of $CD8^+$ T cells were enhanced by immunization with pU-HSP65 but not with pHSP65.

B16F1 melanoma cells expressing Ub-mHSP65 are more immunogenic

Vaccination with plasmid encoding a Ub-fused antigen effectively induces antigen-specific $CD8^+$ T cells by enhanced generation of MHC class I epitopes through UPS in antigen presenting cells, leading us to hypothesize that tumor cells expressing Ub-fused antigens become well recognized by $CD8^+$ T cells specific for the antigens because of enhanced display of antigenic epitopes associated with MHC class I molecules. To test this hypothesis, mice were immunized with pU-HSP65 and transplanted with HSP65/B16F1 or Ub-HSP65/B16F1. In control immunized mice, Ub-HSP65/B16F1 cells grew faster than HSP65/B16F1 (Fig. 4A), indicating that tumorigenicity of Ub-HSP65/B16F1 was higher than that of HSP65/B16F1. Immunization with pU-HSP65 again significantly suppressed the growth of HSP65/B16F1 (Fig. 4A). Surprisingly, this immunization completely suppressed the growth of higher tumorigenic Ub-HSP65/B16F1. Anti-tumor effect of this vaccination against Ub-HSP65/B16F1 was much higher than that against HSP65/B16F1, indicating that immunogenicity of Ub-HSP65/B16F1 was higher than that of HSP65/B16F1.

Our hypothesis is that the high immunogenicity of Ub-HSP65/B16F1 might be contributing to the effective processing and presentation of Ub-mHSP65. To exclude the possibility that the difference of expression of MHC class I molecules is attributable to the different immunogenicity between HSP65/B16F1 and Ub-HSP65/B16F1 cells, we analyzed expression of MHC class I molecules on the surface of those melanoma cells. Low immunogenic B16F10 melanoma cells that express no MHC class I molecules were used as a negative control (Fig. 4B). We found the same expression levels of MHC class I molecules on the surface of parental B16F1, HSP65/B16F1, and Ub-HSP65/B16F1. Taken together, these results strongly suggest that expression of Ub-mHSP65 in tumor cells results in high immunogenicity.

Discussion

Induction of protective $CD8^+$ T cells is one of the final goals for developing effective vaccines and immunity-based therapeutic interventions against infectious diseases as well as against tumors. $CD8^+$ T cells contribute to protection by inducing cytotoxic activity against infected cells and by producing inflammatory cytokines such as IFN-γ. In the present study, vaccination with plasmid DNA encoding Ub-mHSP65 induced anti-tumor immunity against B16F1 melanoma cell expression of mHSP65, as well as eliciting cytotoxic activity and an increase in granzyme B- or IFN-γ-producing $CD8^+$ T cells.

We previously demonstrated that vaccination using DNA encoding a fusion protein between Ub and target antigen is a highly effective strategy for inducing $CD8^+$ T cell-mediated protective immune responses [9–12]. In physiological conditions, attachment of the first Ub to unfolded/harmful proteins occurs under the stringent regu-

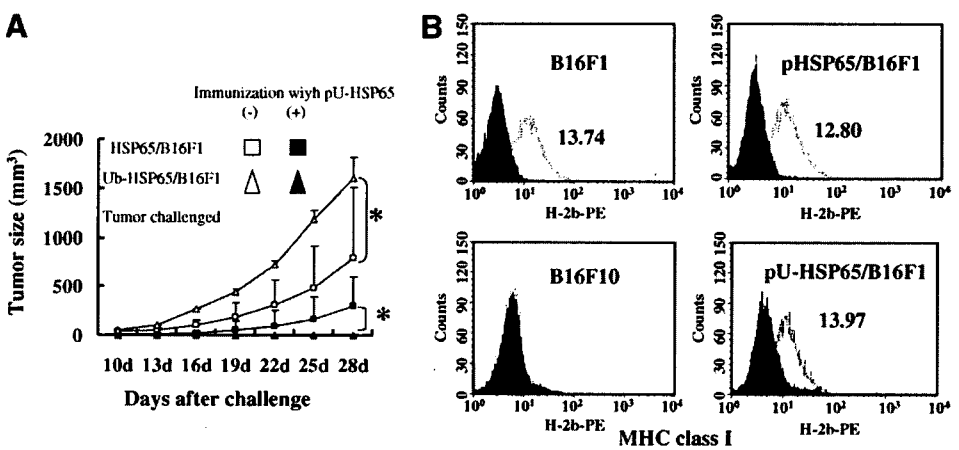

Fig. 4. Immunogenicity of melanoma cells expressing Ub-mHSP65. (A) B6 mice immunized with pDNA (open symbols) or pU-HSP65 (closed symbols) were transplanted with HSP65/B16 (squares) or Ub-HSP65/B16 (triangles). Tumor growth was analyzed as in Fig. 3. Asterisk indicates statistical significance at $P < 0.05$ with the Student's t-test compared with the other group. (B) Expression of MHC class I molecules on the surface of the various melanoma cells as illustrated was analyzed using flow cytometry. The expression profile of MHC class I (broken lines) was plotted against that stained with irrelevant antibody (shaded areas). The numbers represent mean fluorescence intensity.

lation to preferentially degrade those proteins. Once the first Ub is attached to the substrates, the process of polyubiquitination is rapidly initiated. Thus, ubiquitination is the rate-limiting step of protein degradation by UPS. Vaccination with genes encoding artificially Ub-fused antigen are designed to enhance the formation of polyubiquitination of that antigen, resulting in recognition and degradation of the antigen by the proteasomes, which is the first step of antigen processing for $CD8^+$ T cells. Indeed, Ub-mHSP65 transiently expressed in COS-7 cells and stably expressed in B16F1 melanoma cells were promptly degraded by the proteasome compared with those cells that expressed nonubiquitinated mHSP65.

The expression of Ub-mHSP65 effectively induced $CD8^+$ T cells in APCs on vaccination, moreover, it made melanoma cells more immunogenic. The vaccination with pU-HSP65 completely eradicated melanoma cells expressing Ub-mHSP65 which grew well in the unvaccinated host, although the vaccination only suppressed the growth of melanoma cells expressing mHSP65 by around 50% as judged by tumor size. These findings further confirmed that the enhanced antigen presentation to $CD8^+$ T cells was a result of prompt degradation of Ub-mHSP65. It still remains to be seen why expression of Ub-mHSP65 increased melanoma growth. UPS may contribute to maintenance of homeostasis in tumor cells by regulating the turnover of cellular proteins synthesized in association with the rapid cell cycle, as recent reports have demonstrated that proteasome inhibitors are potent anti-tumor drugs [13–15]. Thus, Ub-fused proteins appear to activate UPS.

Although we used the tumor model to evaluate effective activation of $CD8^+$ T cells, our original goal still is to apply this strategy for vaccination against infection with *M. tuberculosis*. Because live vaccination with *M. bovis* (Bacillus Calmette Guerin, BCC) has been shown to be insufficient to prevent the development of tuberculosis, great efforts have been made to develop new vaccines against tuberculosis. However, the results from a range of laboratories using diverse DNA vaccines in diverse infection models have been inconclusive. The importance of $CD8^+$ T cells in protective immunity against tuberculosis has been well documented [1–4,16–19]. For example, mice genetically deficient in β_2-microglobulin, which lack functional MHC class I molecules and consequently $CD8^+$ T cells, fail to control infection with *M. tuberculosis* [16]. Mice deficient in MHC class Ia molecule, CD8 itself, or in TAP are highly susceptible to the infection [17,18]. Jun Wang and colleagues found both $CD8^+$ T cell activation and $CD8^+$ T cell-mediated protection from MT challenge occur in mycobacterial-vaccinated $CD4^+$ T cell-deficient mice [19]. These studies support the idea that stimulation of the $CD8^+$ T cell population must be considered in vaccine design against tuberculosis.

This is the first report suggesting that DNA vaccination with a gene encoding a ubiquitin-fused mHSP65 can potently induce $CD8^+$ T cells specific for mHSP65. This finding may provide a new strategy for designing effective DNA vaccines against *M. tuberculosis*.

Acknowledgment

We thank M. Sano for technical support.

References

[1] J.S. Tan, D.H. Canaday, W.H. Boom, K.N. Balaji, S.K. Schwander, E.A. Rich, Human alveolar T lymphocyte responses to *Mycobacterium tuberculosis* antigens: role for CD4+ and CD8+ cytotoxic T cells and relative resistance of alveolar macrophages to lysis, J. Immunol. 159 (1997) 290–297.

[2] D.M. Lewinsohn, M.R. Alderson, A.L. Briden, S.R. Riddell, S.G. Reed, K.H. Grabstein, Characterization of human CD8+ T cells reactive with *Mycobacterium tuberculosis*-infected antigen-presenting cells, J. Exp. Med. 187 (1998) 1633–1640.

[3] J.S. Woodworth, S.M. Behar, *Mycobacterium tuberculosis*-specific CD8+ T cells and their role in immunity, Crit. Rev. Immunol. 26 (2006) 317–352.

[4] J.E. Grotzke, D.M. Lewinsohn, Role of CD8+ T lymphocytes in control of *Mycobacterium tuberculosis* infection, Microbes Infect. 7 (2005) 776–788.

[5] K. Tanaka, M. Kasahara, The MHC class I ligand-generating system: roles of immunoproteasomes and the interferon-gamma-inducible proteasome activator PA28, Immunol. Rev. 163 (1998) 161–176.

[6] F.J. Doherty, S. Dawson, R.J. Mayer, The ubiquitin-proteasome pathway of intracellular proteolysis, Essays Biochem. 38 (2002) 51–63.

[7] C.M. Pickart, Mechanisms underlying ubiquitination, Annu. Rev. Biochem. 70 (2001) 503–533.

[8] H. Rouard, B. Klonjkowski, J. Marquet, C. Lahet, S. Mercier, M. Andrieu, P. Maison, V. Molinier-Frenkel, M. Eloit, J.P. Farcet, P. Langlade-Demoyen, M.H. Delfau-Larue, Adenoviral transgene ubiquitination enhances mouse immunization and class I presentation by human dendritic cells, Hum. Gene Ther. 14 (2003) 1319–1332.

[9] M. Zhang, K. Ishii, H. Hisaeda, S. Murata, T. Chiba, K. Tanaka, Y. Li, C. Obata, M. Furue, K. Himeno, Ubiquitin-fusion degradation pathway plays an indispensable role in naked DNA vaccination with a chimeric gene encoding a syngeneic cytotoxic T lymphocyte epitope of melanocyte and green fluorescent protein, Immunology 112 (2004) 567–574.

[10] K. Ishii, H. Hisaeda, X. Duan, T. Imai, T. Sakai, H.J. Fehling, S. Murata, T. Chiba, K. Tanaka, S. Hamano, M. Sano, A. Yano, K. Himeno, The involvement of immunoproteasomes in induction of MHC class I-restricted immunity targeting Toxoplasma SAG1, Microbes Infect. 8 (2006) 1045–1053.

[11] M. Zhang, C. Obata, H. Hisaeda, K. Ishii, S. Murata, T. Chiba, K. Tanaka, Y. Li, M. Furue, B. Chou, T. Imai, X. Duan, K. Himeno, A novel DNA vaccine based on ubiquitin-proteasome pathway targeting 'self'-antigens expressed in melanoma/melanocyte, Gene Ther. 12 (2005) 1029–1057.

[12] X. Duan, H. Hisaeda, J. Shen, L. Tu, T. Imai, B. Chou, S. Murata, T. Chima, K. Tanaka, H.J. Fehling, T. Koga, K. Sueishi, K. Himeno, The ubiquitin-proteasome system plays essential roles in presenting an 8-mer CTL epitope expressed in APC to corresponding CD8+ T cells, Int. Immunol. 18 (2006) 679–687.

[13] I. Zavrski, C. Jakob, P. Schmid, H. Krebbel, M. Kaiser, C. Fleissner, M. Rosche, K. Possinger, O. Sezer, Proteasome: an emerging target for cancer therapy, Anticancer Drugs 16 (2005) 475–481.

[14] J. Adams, V.J. Palombella, P.J. Elliott, Proteasome inhibition: a new strategy in cancer treatment, Invest. New Drugs 18 (2000) 109–121.

[15] Y. Ishii, S. Waxman, D. Germain, Targeting the ubiquitin-proteasome pathway in cancer therapy, Anticancer Agents Med. Chem. 7 (2007) 359–365.

[16] J.L. Flynn, M.M. Goldstein, K.J. Triebold, B. Koller, B.R. Bloom, Major histocompatibility complex class I-restricted T cells are required for resistance to *Mycobacterium tuberculosis* infection, Proc. Natl. Acad. Sci. USA 89 (1992) 12013–12017.

[17] A.O. Sousa, R.J. Mazzaccaro, R.G. Russell, F.K. Lee, O.C. Turner, S. Hong, L. Van Kaer, B.R. Bloom, Relative contributions of distinct MHC class I-dependent cell populations in protection to tuberculosis infection in mice, Proc. Natl. Acad. Sci. USA 97 (2000) 4204–4208.

[18] M.S. Rolph, B. Raupach, H.H. Kobernick, H.L. Collins, B. Perarnau, F.A. Lemonnier, S.H. Kaufmann, MHC class Ia-restricted T cells partially account for beta2-microglobulin-dependent resistance to *Mycobacterium tuberculosis*, Eur. J. Immunol. 31 (2001) 1944–1949.

[19] J. Wang, M. Santosuosso, P. Ngai, A. Zganiacz, Z. Xing, Activation of CD8 T cells by mycobacterial vaccination protects against pulmonary tuberculosis in the absence of CD4 T cells, J. Immunol. 173 (2004) 4590–4597.

Epigenetic Silencing of *Plasmodium falciparum* Genes Linked to Erythrocyte Invasion

Alfred Cortés[1,2*], Celine Carret[3], Osamu Kaneko[4¤], Brian Y. S. Yim Lim[1], Alasdair Ivens[3], Anthony A. Holder[1]

1 Division of Parasitology, Medical Research Council National Institute for Medical Research (NIMR), London, United Kingdom, 2 Institució Catalana de Recerca i Estudis Avançats (ICREA) and Institute for Research in Biomedicine (IRB), Barcelona, Catalonia, Spain, 3 Pathogen Microarrays Group, The Wellcome Trust Sanger Institute, Cambridge, United Kingdom, 4 Department of Molecular Parasitology, Ehime University Graduate School of Medicine, Ehime, Japan

The process of erythrocyte invasion by merozoites of *Plasmodium falciparum* involves multiple steps, including the formation of a moving junction between parasite and host cell, and it is characterised by the redundancy of many of the receptor–ligand interactions involved. Several parasite proteins that interact with erythrocyte receptors or participate in other steps of invasion are encoded by small subtelomerically located gene families of four to seven members. We report here that members of the *eba, rhoph1/clag, acbp,* and *pfRh* multigene families exist in either an active or a silenced state. In the case of two members of the *rhoph1/clag* family, *clag3.1* and *clag3.2,* expression was mutually exclusive. Silencing was clonally transmitted and occurred in the absence of detectable DNA alterations, suggesting that it is epigenetic. This was demonstrated for *eba-140.* Our data demonstrate that variant or mutually exclusive expression and epigenetic silencing in *Plasmodium* are not unique to genes such as *var,* which encode proteins that are exported to the surface of the erythrocyte, but also occur for genes involved in host cell invasion. Clonal variant expression of invasion-related ligands increases the flexibility of the parasite to adapt to its human host.

Citation: Cortés A, Carret C, Kaneko O, Yim Lim BYS, Ivens A, et al. (2007) Epigenetic silencing of *Plasmodium falciparum* genes linked to erythrocyte invasion. PLoS Pathog 3(8): e107. doi:10.1371/journal.ppat.0030107

Introduction

Invasion of human erythrocytes by merozoites of the malaria parasite *P. falciparum* is an essential step of the asexual blood cycle of the parasite, which is responsible for all the pathology associated with the disease. Erythrocyte invasion by merozoites of *P. falciparum* is relatively well characterised at the ultrastructural level [1], but the precise molecular interactions and the role of the specific parasite proteins are still poorly described. Proteins located on the surface of the merozoite probably mediate the initial, reversible contact through low affinity interactions. The next step involves reorientation of the merozoite, such that its apical end, which contains specialised organelles like rhoptries and micronemes, faces the erythrocyte. This is followed by the irreversible formation of a tight moving junction based on high affinity interactions (reviewed in [2]). The micronemal protein EBA-175 is believed to participate in junction formation by interacting with the erythrocyte surface protein glycophorin A [3], but other proteins located in the apical organelles of the merozoite are also likely to be involved. Strong candidates are the proteins encoded by the small gene families *eba* (also known as *dbl-ebp,* to which *eba-175* belongs) and *pfRh* (also known as *pfnbp* or *pfrbl*), and recent data suggest that some members of the two families may have overlapping roles [4]. All individual members of these two gene families seem to be non-essential, as they can be knocked out without impairing parasite growth (reviewed in [2]). AMA1 and thrombospondin repeat domain–containing proteins may also play a role in the formation or migration of the junction [2]. Whatever the precise proteins involved, it is clear that there is redundancy in many of the ligand–receptor interactions between the apical end of the parasite and the erythrocyte. The particular set of receptor–ligand interactions used for invasion determine the so-called alternative invasion pathways, which are described by the sensitivity of invasion to treatment of erythrocytes with various enzymes. It is well established that both field isolates and laboratory-adapted parasite lines vary in their capacity to use the different invasion pathways [5,6].

In the next stage of invasion, the junction migrates towards the posterior end of the parasite driven by a parasite actin-myosin motor, creating an invagination in the erythrocyte membrane. The final step is the sealing of the invagination, which forms a parasitophorous vacuole where the parasite will reside until the next cycle of invasion. Although it is not well established which proteins participate in the formation of the vacuole and remodelling of the erythrocyte, it is possible that the high molecular mass rhoptry complex (RhopH complex) has a role [7], in addition to a possible role at earlier stages of invasion. Two of the components of this trimeric complex, RhopH2 and RhopH3, are encoded by single copy genes, whereas RhopH1/Clag can be encoded by five different genes of the *clag* gene family [8].

We recently described two essentially isogenic parasite

Editor: Joe D. Smith, Seattle Biomedical Research Institute, United States of America

Received March 9, 2007; **Accepted** June 11, 2007; **Published** August 3, 2007

Abbreviations: IFA, immunofluorescence assay; ORF, open reading frame; RT-PCR, reverse transcriptase PCR

* To whom correspondence should be addressed. E-mail: acortes@pcb.ub.es

¤ Current address: Department of Protozoology, Nagasaki University, Institute of Tropical Medicine, Sakamoto, Nagasaki, Japan